Review of Scientific Instruments

First operation in SPIDER and the path to complete MITICA

Cite as: Rev. Sci. Instrum. **91**, 023510 (2020); https://doi.org/10.1063/1.5133076
Submitted: 26 October 2019 . Accepted: 22 January 2020 . Published Online: 14 February 2020

G. Serianni, V. Toigo, M. Bigi, M. Boldrin, G. Chitarin, S. Dal Bello, L. Grando, A. Luchetta, D. Marcuzzi, R. Pasqualotto, N. Pomaro, P. Zaccaria, L. Zanotto, P. Agostinetti, M. Agostini, V. Antoni, D. Aprile, M. Barbisan, M. Battistella, M. Brombin, A. Canton, R. Cavazzana, M. Dalla Palma, M. Dan, R. Delogu, A. De Lorenzi, M. De Muri, S. Denizeau, M. Fadone, F. Fellin, A. Ferro, E. Gaio, G. Gambetta, F. Gasparini, F. Gnesotto, P. Jain, A. Maistrello, G. Manduchi, S. Manfrin, G. Marchiori, N. Marconato, M. Moresco, T. Patton, M. Pavei, S. Peruzzo, N. Pilan, A. Pimazzoni, R. Piovan, C. Poggi, M. Recchia, A. Rigoni, A. Rizzolo, G. Rostagni, E. Sartori, M. Siragusa, P. Sonato, E. Spada, S. Spagnolo, M. Spolaore, C. Taliercio, P. Tinti, M. Ugoletti, M. Valente, A. Zamengo, B. Zaniol, M. Zaupa, M. Cavenago, D. Boilson, C. Rotti, P. Veltri, J. Chareyre, H. Decamps, M. Dremel, J. Graceffa, F. Geli, B. Schunke, L. Svensson, M. Urbani, T. Bonicelli, G. Agarici, A. Garbuglia, A. Masiello, F. Paolucci, M. Simon, L. Bailly-Maitre, E. Bragulat, G. Gomez, D. Gutierrez, C. Labate, G. Mico, J. F. Moreno, V. Pilard, G. Kouzmenko, A. Rousseau, A. Chakraborty, U. Baruah, H. Patel, N. P. Singh, A. Patel, H. Dhola, B. Raval, S. Cristofaro, U. Fantz, B. Heinemann, W. Kraus, M. Kashiwagi, and H. Tobari

AIP Publishing

Review of Scientific Instruments ARTICLE scitation.org/journal/rsi

First operation in SPIDER and the path to complete MITICA

Cite as: Rev. Sci. Instrum. 91, 023510 (2020); doi: 10.1063/1.5133076
Submitted: 26 October 2019 • Accepted: 22 January 2020 •
Published Online: 14 February 2020

G. Serianni,[1,a)] V. Toigo,[1] M. Bigi,[1] M. Boldrin,[1] G. Chitarin,[1,2] S. Dal Bello,[1] L. Grando,[1] A. Luchetta,[1] D. Marcuzzi,[1] R. Pasqualotto,[1] N. Pomaro,[1] P. Zaccaria,[1] L. Zanotto,[1] P. Agostinetti,[1] M. Agostini,[1] V. Antoni,[1] D. Aprile,[1,3] M. Barbisan,[1] M. Battistella,[1] M. Brombin,[1] A. Canton,[1] R. Cavazzana,[1] M. Dalla Palma,[1] M. Dan,[1] R. Delogu,[1] A. De Lorenzi,[1] M. De Muri,[1] S. Denizeau,[1] M. Fadone,[1] F. Fellin,[1] A. Ferro,[1] E. Gaio,[1] G. Gambetta,[1] F. Gasparini,[1] F. Gnesotto,[1] P. Jain,[1] A. Maistrello,[1] G. Manduchi,[1] S. Manfrin,[1] G. Marchiori,[1] N. Marconato,[1] M. Moresco,[1] T. Patton,[1] M. Pavei,[1] S. Peruzzo,[1] N. Pilan,[1] A. Pimazzoni,[1,3] R. Piovan,[1] C. Poggi,[1] M. Recchia,[1] A. Rigoni,[1] A. Rizzolo,[1] G. Rostagni,[1] E. Sartori,[1,2] M. Siragusa,[1] P. Sonato,[1] E. Spada,[1] S. Spagnolo,[1] M. Spolaore,[1] C. Taliercio,[1] P. Tinti,[1] M. Ugoletti,[1] M. Valente,[1] A. Zamengo,[1] B. Zaniol,[1] M. Zaupa,[1] M. Cavenago,[3] D. Boilson,[4] C. Rotti,[4] P. Veltri,[4] J. Chareyre,[4] H. Decamps,[4] M. Dremel,[4] J. Graceffa,[4] F. Geli,[4] B. Schunke,[4] L. Svensson,[4] M. Urbani,[4] T. Bonicelli,[5] G. Agarici,[5] A. Garbuglia,[5] A. Masiello,[5] F. Paolucci,[5] M. Simon,[5] L. Bailly-Maitre,[5] E. Bragulat,[5] G. Gomez,[5] D. Gutierrez,[5] C. Labate,[5] G. Mico,[5] J. F. Moreno,[5] V. Pilard,[5] G. Kouzmenko,[5] A. Rousseau,[5] A. Chakraborty,[6] U. Baruah,[6] H. Patel,[6] N. P. Singh,[6] A. Patel,[6] H. Dhola,[6] B. Raval,[6] S. Cristofaro,[7] U. Fantz,[7] B. Heinemann,[7] W. Kraus,[7] M. Kashiwagi,[8] and H. Tobari[8]

AFFILIATIONS

[1]Consorzio RFX (CNR, ENEA, INFN, UNIPD, Acciaierie Venete SpA), Corso Stati Uniti 4, 35127 Padova, Italy
[2]Dept. of Management and Engineering, Università degli Studi di Padova, Strad. S. Nicola 3, 36100 Vicenza, Italy
[3]INFN-Laboratori Nazionali di Legnaro (LNL), v.le dell'Università 2, I-35020 Legnaro, PD, Italy
[4]ITER Organization, Route de Vinon-sur-Verdon, CS 90 046, F-13067 St. Paul-lez-Durance, France
[5]Fusion for Energy, C/o Josep Pla 2, E-08019 Barcelona, Spain
[6]ITER-India, Institute for Plasma Research, Nr. Indira Bridge, Bhat Village, Gandhinagar, Gujarat 382428, India
[7]IPP, Max-Planck-Institut für Plasmaphysik, Boltzmannstraße 2, D-85748 Garching bei München, Germany
[8]National Institutes for Quantum and Radiological Science and Technology, 801-1 Mukoyama, Naka, Ibaraki-ken 311-0193, Japan

Note: Invited paper, published as part of the Proceedings of the 18th International Conference on Ion Sources, Lanzhou, China, September 2019.
[a)]**Author to whom correspondence should be addressed:** gianluigi.serianni@igi.cnr.it

ABSTRACT

The requirements of ITER neutral beam injectors (1 MeV, 40 A negative deuterium ion current for 1 h) have never been simultaneously attained; therefore, a dedicated Neutral Beam Test Facility (NBTF) was set up at Consorzio RFX (Padova, Italy). The NBTF includes two experiments: SPIDER (Source for the Production of Ions of Deuterium Extracted from Rf plasma), the full-scale prototype of the source of ITER injectors, with a 100 keV accelerator, to investigate and optimize the properties of the ion source; and MITICA, the full-scale prototype of the entire injector, devoted to the issues related to the accelerator, including voltage holding at low gas pressure. The present paper gives an account of the status of the procurements, of the timeline, and of the voltage holding tests and experiments for MITICA. As for SPIDER, the first year of operation is described, regarding the solution of some issues connected with the radiofrequency power, the source operation, and the characterization of the first negative ion beam.

I. INTRODUCTION

To reach fusion conditions and to control the plasma configuration in ITER, which represents the next step in controlled thermonuclear fusion research, two heating and current-drive neutral beam injectors (NBIs) will supply a total power of 33 MW, by accelerating negative deuterium ions to 1 MeV.[1] The requirements of ITER NBIs, in terms of negative ion current (40 A) and beam-on time (1 h) have never been simultaneously attained. Because of this, in the dedicated Neutral Beam Test Facility (NBTF) at Consorzio RFX (Italy) the performances of the ITER NBI (including the beam optics) will be studied and optimized.[2–4] The NBTF includes two experiments: MITICA,[5] the full-scale ITER NBI prototype, and SPIDER (Source for the Production of Ions of Deuterium Extracted from Rf plasma),[6] the full-scale prototype of the ITER NBI source with 100 keV particle energy. SPIDER's goal is to investigate and optimize the uniformity of the source plasma (over a 1 m × 2 m area), the current density of the negative ions, and to study the beam optics at low energy.[7] When MITICA exploitation will begin, the experience gained in SPIDER will be immediately applied to the operation of the ion source; SPIDER will continue to operate to address source-specific topics in view of the ITER NBI and MITICA will be employed to solve the issues related to the accelerator, including beam optics in ITER-relevant conditions and high voltage holding in vacuum. This way the NBTF will provide several years of experience with the source and the whole injector before the start of ITER NBI and will accompany the ITER NBI operation so as to solve possible injector issues.[2] Thus, the NBTF schedule is tightly linked with the overall ITER staged approach,[8] which assumes both ITER NBIs to be installed by September 2031. To fulfill such a plan, SPIDER is required to provide most of the relevant information when MITICA will start beam operation (spring 2023), whereas the experience gained with SPIDER and MITICA will have to confirm the design of the beam source of ITER NBIs, whose construction is planned to start by mid-2027.

The present contribution will briefly outline the activities and the experiments carried out in SPIDER during its first year of operation with volume generation of negative hydrogen ions, including the first investigation of a negative ion beam in SPIDER. Moreover, an update will be given about the status of MITICA and of the whole NBTF as well as a brief outline of the activities planned for the near future, both for SPIDER and MITICA.

II. SPIDER OPERATIONS

The SPIDER experiment is the full-size plasma source of MITICA (see Sec. III) and of the NBI for ITER; source operation was started in May 2018.[7] The design parameters are summarized in Table I. The SPIDER ion source design[9] is essentially the same as that for MITICA: the plasma is generated inductively by eight coils powered in pairs by four radiofrequency (RF) generators and provides up to 200 kW each. The plasma expands into a chamber, which is closed, opposite to the drivers, by the plasma grid (PG), provided with 1280 apertures, arranged into 4 × 4 groups. Each group features 5(horizontally) × 16(vertically) apertures, through which negative ion beamlets are extracted, thanks to the electrostatic field induced by the voltage difference applied with respect to the next grid [extraction grid (EG)]. Finally, the voltage applied with respect to the last grid [grounded grid (GG)] accelerates particles up to the total energy of about 100 keV. In accelerators of negative ions, electrons are co-extracted from the plasma together with the negative ions; a suitable arrangement of permanent magnets, housed in the EG, dumps the electrons onto the EG itself; this field however affects also the trajectories of negative ions so that suitable countermeasures are needed to compensate for such negative ion deflection. The whole magnetic field configuration of SPIDER shares the basic principles with MITICA; in both cases, the compensation of the negative ion deflection is performed by another system of permanent magnets, which are embedded in the EG itself[10] for MITICA and in the GG for SPIDER (which also requires a ferromagnetic plate on the downstream side of the GG). In both devices, a magnetic filter field is created just upstream with respect to the PG by currents flowing in the PG and in other busbars, in order to reduce the temperature and the density of electrons in the vicinity of the PG and hence the lifetime and density of negative ions. In negative ion beams, the amount of negative ions in the PG region is greatly enhanced by cesium-catalyzed conversion of positive hydrogen ions and atoms impinging on the PG. To this purpose, dedicated evaporators (not yet operating in SPIDER) inject cesium into the ion source.[11]

TABLE I. Main design parameters of SPIDER.

Parameter	Value
Beam energy (keV)	100
Max source filling pressure (Pa)	0.3
Max deviation from beam uniformity	±10%
Extracted ion current density (A/m^2)	>355 H_2; >285 D_2
Beam on time	1 h
Co-extracted electron fraction	<0.5 (H_2); <1 (D_2)

SPIDER is a key asset in the development of the negative-ion beam source for ITER. For the first time, the vacuum-insulated source concept is fully applied to a beam source for fusion: the multi-aperture multi-electrode electrostatic accelerator and the RF-driven plasma source (at high voltage) are completely contained in the same vacuum as the beam drift region (Fig. 1). Electrical insulation from the vessel is achieved by maintaining a sufficiently low gas pressure to avoid electrical discharges in the Paschen region. Unlike the other existing prototype sources for fusion applications, SPIDER allows us to develop procedures and technical solutions that are specific of this vacuum-insulated source concept. In this sense, during the first year of operation, the experimental activities addressed a pressing issue related to electrical insulation in the presence of RF fields, a condition that is more difficult than in the steady state. More than one year since the ignition of the first plasma and after a large effort dedicated, in parallel, to the commissioning of diagnostics and to the optimization of the RF generators, SPIDER routinely operates the negative-ion beam produced in the plasma volume. Presently, the experimental work focusses on concluding the commissioning and on improving the reliability of all SPIDER plants, in view of cesium operation. The vacuum-insulated source concept indeed does not allow accessing any part of the beam source for maintenance or mechanical improvements, without breaking the same vacuum in which the cesium layer is built up and conditioned for negative ion production.

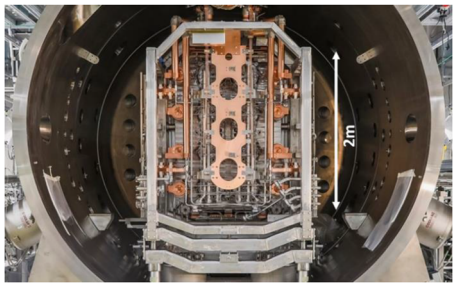

FIG. 1. Rear view of SPIDER beam source in vacuum vessel.

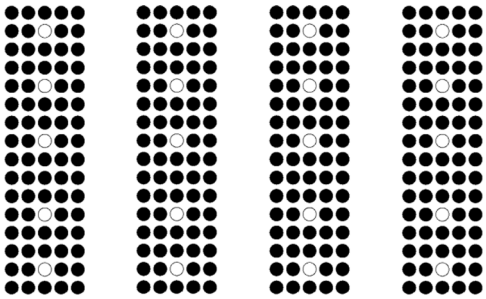

FIG. 2. Arrangement of apertures in the segments of the SPIDER accelerator grids. White circles indicate operating beamlets.

A. Identification of a solution for the RF-induced discharges

During SPIDER operations in 2018,[7] two interrelated issues emerged, regarding the difficulty in increasing the RF power applied to the RF coils and the occurrence of RF-induced discharges on the rear side of the beam source.[12] These issues impeded simultaneous operation of all RF drivers as well as the operation above a total RF power of ~100 kW. A strategy was developed to identify and address the cause of the problem. Based on the experience of the ELISE test facility,[13] the cause might be the triple points between different materials, where RF electric fields develop, which can induce breakdowns at large RF power. On the other hand, the very RF voltage at components of the resonant circuit (the matching network that is located on the rear side of the source, namely, in vacuum) can induce breakdowns at unfavorable gas pressures. It was decided to verify whether the latter was the primary cause, by designing an experiment with reduced vessel pressure within a wide range of source pressures. This was attained by installing a plate inside the accelerator so as to close all the apertures of the EG, resulting in a drastic reduction of the gas conductance from the source to the vessel. This experiment showed that in the present operating conditions (up to ~100 kW per generator), the dominant effect is related to the gas pressure: it was recognized that above a vessel pressure of 40 mPa, the probability of discharges quickly increases; without the plate, such a pressure would correspond to only 0.1 Pa inside the ion source. In parallel to the definition of a long-term major modification of SPIDER pumping system, (to this purpose also non-evaporable getters are being considered[14]), it was decided to carry on with the experimental program, upon reducing the gas conductance between the source and the vessel by installing a mask on the downstream side of the plasma grid. The mask features 80 apertures (out of 1280); Fig. 2 shows the aperture arrangement in each grid segment (corresponding to 1/4 of a grid). The computation method adopted to model the gas pressure profile, based on the view factor technique, is described in Ref. 15, the mechanical design and installation can be found in Ref. 16, and the electrical considerations and tests are exposed in Ref. 17.

B. Source and beam characterization

After a shutdown started at the end of November 2018, including the installation of the plasma grid mask, SPIDER operations resumed at mid-April 2019 and were devoted to the following activities: characterization of the RF circuits; characterization of the ion source; testing of the extraction and accelerator power supplies; and first characterization of the SPIDER beam. As of 2019, most of SPIDER diagnostic systems[18] are operating: the list of source diagnostics[19] include source emission spectroscopy, surface and calorimetry thermocouples, H_{alpha} detectors, visible cameras, and electrical measurements at the various power supplies. The electrostatic sensors embedded in the plasma grid and in the bias plate[20] are under commissioning; the diagnostic systems more tightly related with the cesium operation, like laser absorption spectroscopy[21] and cavity ring-down spectroscopy, will soon be installed and commissioned. The operating diagnostic systems allowed the measurement of the plasma and beam parameters in different experimental conditions, which can be explored even within single pulses thanks to the very flexible SPIDER control system;[22] an overview of the results of the experimental campaigns is given in the following.

A first characterization of the RF circuits was carried out in parallel to the implementation of a feedforward control of the internal capacitors of the RF generators and to the development of a model reproducing the behavior of the RF system. The experiments focused on the parallel capacitance of the matching network, after the temporary installation of different capacitors on the four circuits (5 nF, 6.5 nF, 10 nF, and 15 nF). The experiments confirmed the presence of hysteresis resulting in a "forbidden" region of frequencies (unfortunately, the optimal frequency for transfer of RF to the coils lies in this region) and provided a benchmark for the numerical simulations of the RF circuits. Thus, it was possible to thoroughly assess the features of the generators, although in single-generator operation only, so as to attain an RF power per generator up to 125–145 kW (depending on the generator). Based on this campaign and on the numerical codes, it was subsequently possible to simultaneously and reliably operate the four RF generators up to 100 kW per generator, after restoring the original 10 nF parallel capacitance of all matching networks. Increasing the RF power above that value will be the subject of further investigations (Sec. II C).

As for the characterization of the ion source, signals from H_{alpha} detectors[23] and emission spectra[24] indicate that, both in the drivers and close to the plasma grid, the plasma emission increases with RF power. The plasma completely fills the drivers and the expansion chamber; the plasma emission seems to be slightly larger at the bottom of the ion source, but this statement deserves further

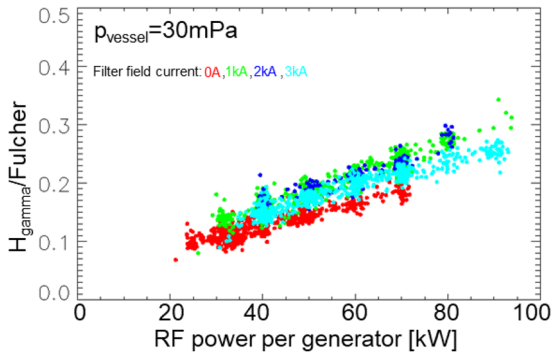

FIG. 3. Ratio of H_{gamma} and Fulcher brightness vs RF power for different values of the magnetic filter field current.

investigation. The ratio between H_{gamma} and the Fulcher band seems to increase with the RF power (Fig. 3), suggesting a corresponding increase of the dissociation degree of hydrogen. The rotational temperature of the hydrogen molecules increases with RF power and gas pressure. No major influence of electron and beam extraction on the plasma surrounding the PG is suggested by spectroscopy (but it shall be remembered that no cesium was used in SPIDER to enhance the negative ion amount yet). The magnetic filter field was found to affect the plasma even far away from the plasma grid; the light emitted by the plasma reaches a maximum for a certain value of the filter field current (between 600 A and 1500 A, depending on pressure and RF power) and decreases for larger values (at low RF power the plasma can be even switched off for large filter field). This evidence was ascribed to the specific topology of the magnetic filter field, which features magnetic field lines intersecting the walls of the RF drivers, thus distorting the electron trajectories, as confirmed by the increase of the heat deposited onto these surfaces as the filter field increases. The magnetic configuration will be improved in the future (Sec. II C).

The first negative ion beam was extracted from the SPIDER ion source and accelerated at the end of May 2019. The signature of the negative hydrogen beam can be clearly seen by the light emitted when the beam interacts with the background gas (Fig. 4, left). Afterward, a first characterization was performed of the beam features and of the amount of co-extracted electrons. The bias voltages applied to plasma grid and to bias plate were found to affect the amount of co-extracted electrons. Combination of the two voltages, such that the bias plate is slightly more positive than the plasma grid, seems more effective (due to the presently limited voltage range of the bias power supplies, these experiments were performed only at low RF power; this voltage limitation will soon be removed, as described in Sec. II C). As in other devices,[25] co-extracted electrons decrease with an increase in gas pressure. The magnetic filter field is found to selectively reduce the amount of co-extracted electrons with respect to the negative ions.

The SPIDER beam features can be studied by means of several diagnostic systems: apart from the electrical measurements provided by the power supplies, dedicated diagnostics include visible cameras (constituting the first set of cameras of the beam tomographic system[26]), beam emission spectroscopy and the Short-Time Retractable Instrumented KalorimEter (STRIKE);[27] an emittance scanner is also under preparation.[28,29] The electrical measurement of the beam current at the accelerator power supply, and the electrical current collected by STRIKE (located at 0.7 m from the grounded grid) were found to be comparable and to increase with the extraction voltage (Fig. 5). The current equivalent to the beam energy flux measured calorimetrically at STRIKE confirms the same trend. As expected, the calorimetrical estimate of the negative ion current is lower than the electrical measurement because the latter includes some of the secondary electrons belonging to the plasma generated by the interaction of the negative ion beam with the background gas. Interpreting the specific value of the ratio between the two estimates (Fig. 5 shows a factor of 2.5 during this first beam characterization) requires numerical simulations of the beam plasma, which will be addressed in the future.

The installation of the plasma grid mask in SPIDER leaves only isolated beamlets, for a total number of 80 beamlets out of 1280. This configuration of the accelerator gives a unique, albeit temporary,

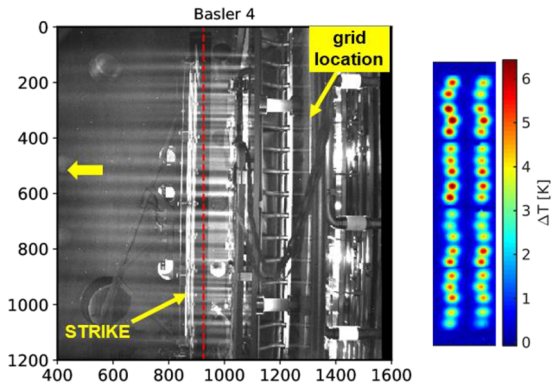

FIG. 4. Image of the beam provided by the visible camera (left); the positions of STRIKE and of the accelerator grids are indicated; and the arrow indicates the beam direction. Footprint of the beamlets onto the STRIKE tiles (right).

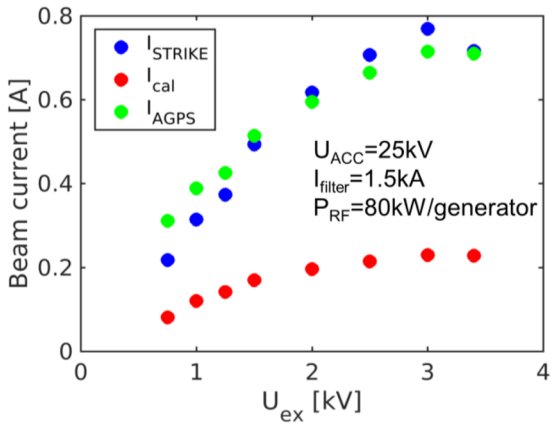

FIG. 5. Dependence of the electrical beam currents (measured at the power supply and on the STRIKE tiles) and of the equivalent calorimetrical current on the extraction voltage.

opportunity for the detailed investigation of the beamlet properties. The beam divergence can be measured in SPIDER by several diagnostic systems. Many visible cameras are installed on the vacuum vessel in different positions and with a different field of view (Fig. 4, left); the Doppler-shifted light emitted by the beam particles is measured by beam emission spectroscopy along several lines-of-sight; the STRIKE calorimeter records the thermal footprints of the single beamlets on the carbon-fiber-carbon composite (CFC) tiles (Fig. 4, right). Similar values of the beamlet divergence, down to 20–30 mrad,[27] were estimated by the various beam diagnostics and the same dependency on the extraction voltage was found.

C. Future experimental plan (end of 2019–2020)

In the fourth quarter of 2019 and in 2020, until the 2020 shutdown, SPIDER experiments will aim at cesium operation and its preparation. A milestone toward cesium operation is the commissioning and testing of all and each of the three cesium ovens. Cesium evaporation from each cesium oven is being demonstrated and characterized[30] in the dedicated facility CAesium Test Stand (CATS).[11] In the next phase, a functional test of the ovens installed in SPIDER is planned, to demonstrate the reliability of the mechanical and electrical design, despite the high voltage and RF environment. Like MITICA and the NBI for ITER, wiring and feedthroughs for the cesium ovens lie beside high voltage and RF connections in the transmission line connecting the source to the high voltage deck (HVD).

An RF optimization campaign will exploit the installation of a variable capacitor and will aim at searching for the maximum RF power attainable with fine control of the capacitance of the matching network (single-generator operation) and at comparing and improving the numerical models of the RF circuitry. Subsequently, strategies to increase the maximum reliable RF power with four generators operating simultaneously will be tested.

As already discussed in Sec. II B, presently, the specific configuration of the magnetic filter field of SPIDER, which exhibits an X-point inside the RF drivers, globally affects the plasma; at the beginning of 2020, the filter field will be improved. Moreover the range of the bias voltages (for plasma grid and bias plate) will be increased to make it suitable also for operation with the volume generation of negative ions, which is characterized by a higher plasma potential. Then, the source parameters will be investigated in detail by introducing a movable system of electrostatic sensors (single and double Langmuir probes, Mach probes, and retarding field energy analysers) and by adding impurities to the process gas. A campaign will be specifically devoted to the study of the deuterium plasma. A second investigation will be carried out of the electron and beam features as functions of the control parameters (RF power, gas pressure, magnetic filter field, bias voltages, and process gas).

In addition to these investigations, the following activities are planned specifically to prepare the cesium operation: the definition of a regeneration procedure for cryogenic pumps minimizing cesium layer pollution, the definition of a reliable high voltage conditioning procedure for the accelerator, the commissioning of the cooling of the beam dump, the commissioning of laser absorption and of cavity ring-down spectroscopy, the demonstration that a cumulative beam and source pulse length per day suitable for a good source cesiation can be attained, and the demonstration of plasma grid temperature control to maintain it at about 150 °C during the cesium operation. In parallel, the caesium-related diagnostic systems are being tested in the CATS facility[31] and simulations of the expected behavior of the cesium evaporators[32] and of cesium dynamics in vacuum are being carried out.[33]

The cesium campaign will be divided into two parts. First, the experimental program will aim at verifying the improvement of the SPIDER performances as cesium is injected. Particularly, investigations will address the effect of the cesium injection rate and conditioning procedure since these parameters are probably specific for a source design and size; the recovery after overnight and weekend breaks will also be assessed. The recovery after cryogenic pump regeneration will necessarily be studied, because, similarly to the ITER NBIs, SPIDER is the first negative-ion source not including an absolute valve to isolate a well-conditioned cesiated source from the vacuum vessel, in which cryogenic pumps are regenerated. Finally, after a sufficient increase of negative ion current and a sufficiently reduced co-extracted electron current is be attained, the experimentation will be devoted to the study of the influence on the beam features of extraction voltage, RF power, gas pressure, process gas (hydrogen and deuterium), bias voltages (plasma grid and bias plate), and strength of the magnetic filter field.

III. STATUS OF MITICA

MITICA is the full-scale injector prototype for ITER NBIs and is expected to demonstrate the operation of the whole ITER injector.[34] It represents a large leap forward in terms of beam power and particle energy with respect to the existing NBIs. The main MITICA parameters are given in Table II: except for the duration of the hydrogen pulses, they correspond to the parameters of the ITER NBIs, as indicated.

MITICA shall provide the particles with 1 MeV total energy; its physics design is described in Ref. 35, and the status as of 2018 was reported in Ref. 36. The components of the MITICA injector are shown in Fig. 6. The MITICA ion source is essentially the same as for SPIDER (see Sec. II). The accelerator is composed of 5 stages, 200 kV each, up to the total particle energy. The magnetic field configuration of MITICA shares the basic principles with SPIDER, although the compensation of the negative ion deflection is performed by another system of permanent magnets embedded in the EG itself.[10]

Herein, a short account will be given of the main procurement advancements. The MITICA vessel is made of two components,

TABLE II. Main design parameters for MITICA; the difference with the ITER NBI is indicated.

Parameter	Value
Beam energy (keV)	1000 (D_2); 870 (H_2)
Max source filling pressure (Pa)	0.3
Beamlet divergence (mrad)	≤7
Accelerated current (A)	46 H_2; 40 D_2
Beam on time	1 h (H_2 in ITER: 1000 s)
Co-extracted electron fraction	<0.5 in H_2; <1 in D_2

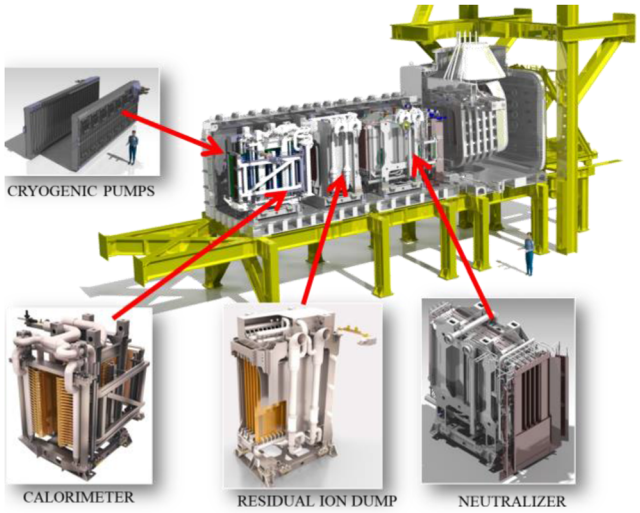

FIG. 6. Structure of the MITICA injector. The beam line components, neutralizer, and residual ion dump are highlighted; the beam source (see Fig. 8) can be seen on the right-hand side. The cryogenic pumps are also sketched.

housing the beam source and the beam line components, respectively (Fig. 7). The beam source vessel (Fig. 7, left) was delivered to the NBTF in spring 2019. It was later installed in its final position and provided with a temporary pumping system; the leak test was successfully performed. As for the beam source, which includes the ion source and the accelerator (Fig. 8), the supply contract was signed with the consortium Alsyom-Seiv (France) in October 2018. The first prototypes of the most critical components of the accelerator (Fig. 9, left) are under construction; an instance of a grid support prototype is shown in Fig. 9, right. The beam source should be delivered to the NBTF by mid-2022.

MITICA beam line includes the following (Fig. 6): the neutralizer, where negative ions are stripped of their additional electrons by passing through a gas cell; the residual ion dump, to dispose of the negative ions that were not neutralized or which underwent double stripping, resulting in positively charged ions; and the calorimeter, which receives the neutral beam power for the entire duration of the MITICA experimentation. Moreover, two large cryogenic pumps are located on either side of the beam line components to provide the

FIG. 7. MITICA beam source vessel under the leak test (left) and the MITICA beam line vessel under construction (right).

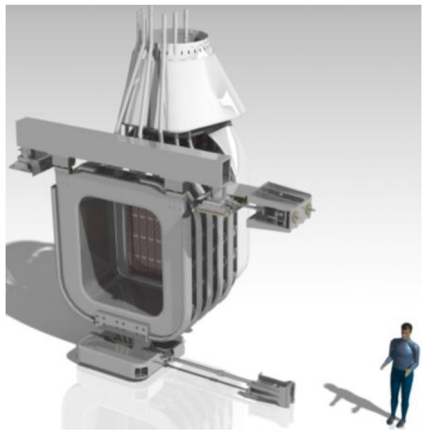

FIG. 8. CAD view of the MITICA beam source.

required vacuum conditions in the vessel ($p_{vessel} < 20$ mPa). The supply of the beam line components involves a two-stage contract: stage 1, devoted to the identification of the supplier companies capable of performing the task, is completed; during this stage, prototypes of some of the most critical components were realized. These suppliers will compete for stage 2, which is under assignment; the delivery of the components is planned for the third quarter of 2023.

The 1 MV power supplies (procured in-kind by the Japanese Domestic Agency) are already installed;[37,38] insulation tests and commissioning have started in 2018 and will be concluded with the insulating test of the whole transmission line, including high voltage bushing and vacuum vessel, scheduled for November 2019. The HVD, housing all power supplies at the source potential (including the RF generators), was provided by F4E. In 2019, the combined tests were performed involving the HVD, the 1 MV power supplies, and the high voltage transformer (required by the devices housed in the HVD): the integrated insulation tests were successfully performed in July 2019 and consisted of the following steps: −1.2 MV for 1 h: −1.06 MV for 5 h and 5 pulses from −1.06 MV to −1.265 MV. In 2020, the following activities will be performed: power integrated tests of the 1 MV power supplies (AGPS) at full

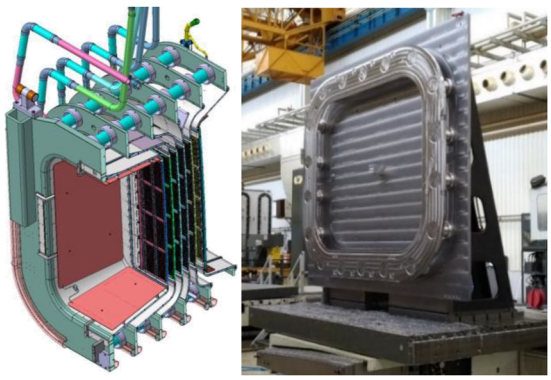

FIG. 9. Cut view of the MITICA accelerator (left). The prototype of the supporting flange of the fourth grid of the MITICA accelerator (right).

power on dummy load; the completion of commissioning and site acceptance tests of the ion source and extraction power supplies (ISEPS), AGPS-ISEPS power integrated tests, and installation and site acceptance tests of the MITICA beam line vessel. In parallel, commissioning and site acceptance tests of the gas and vacuum system will be carried out along with the integration of the plant with the control and protection systems. Starting from 2020, the MITICA power supplies and the vessel, together with an electrostatic mock-up of the source, will be employed to gain experience on high voltage holding in vacuum and at low gas pressure, which is one of the main issues to be addressed in MITICA. Later on, after installing the MITICA beam source inside the vessel, the plasma will be started and characterized in different operational conditions by applying the expertize gained in SPIDER. After delivery and installation of beam line components, the beam operation will start.

IV. ACCOMPANYING FACILITIES

The experimental plan in SPIDER and MITICA is supplemented by an accompanying program, including some small test facilities at the NBTF. The High Voltage RadioFrequency Test Facility (HVRFTF)[39] is devoted to the characterization of the dielectric strength in vacuum of the RF drivers, to address potential voltage holding issues of beam source components under RF electric fields at low gas pressure. In the CAesium Test Stand (CATS)[11] the characterization of the cesium ovens before installation into SPIDER and MITICA is performed, in terms of diagnostics, oven maintenance, and cesium management. The High Voltage Padova Test Facility (HVPTF)[40] aims at performing optimized experiments of voltage holding up to 1 MV in vacuum and with gas, with tight control of voltage, current, pressure, and vacuum quality. The Negative Ion Optimization facility, phase 1 (NIO1),[41] is a versatile multiaperture hydrogen source, with compact and modular design, capable of continuous operation to reproduce the physics conditions of much larger ion sources so as to readily verify the effects of individual source components/parameters and to compare results with simulations.

V. SUMMARY

In this paper, a summary of the activities performed at the ITER neutral beam test facility is given. The components of the MITICA device are being procured or have already been delivered; the 1 MV power supplies are being employed for the voltage holding tests that will soon involve a mock-up of the beam source. The SPIDER facility has been operating with volume generation of negative ions for more than one year. Several issues were addressed and solved, which allowed the acceleration of negative ions beams. Cesium will soon be injected in SPIDER to improve the beam performances.

ACKNOWLEDGMENTS

The work leading to this publication has been funded partially by Fusion for Energy (F4E). This publication reflects the views only of the authors, and F4E cannot be held responsible for any use which may be made of the information contained therein. The views and opinions expressed herein do not necessarily reflect those of the ITER organization.

REFERENCES

[1] T. Inoue *et al.*, Fusion Eng. Des. **56-57**, 517 (2001).
[2] R. H. S. Hemsworth *et al.*, Rev. Sci. Instrum. **79**, 02C109 (2008).
[3] V. Toigo *et al.*, New J. Phys. **19**, 085004 (2017).
[4] L. Grisham, Fusion Eng. Des. **87**, 1805 (2012).
[5] V. Toigo *et al.*, Nucl. Fusion **55**, 083025 (2015).
[6] D. Marcuzzi *et al.*, Fusion Eng. Des. **85**, 1792 (2010).
[7] G. Serianni *et al.*, Fusion Eng. Des. **146**, 2539 (2019).
[8] B. Bigot, Nucl. Fusion **59**, 112001 (2019).
[9] P. Agostinetti *et al.*, Nucl. Fusion **51**, 063004 (2011).
[10] G. Chitarin *et al.*, Rev. Sci. Instrum. **85**, 02B317 (2014).
[11] A. Rizzolo *et al.*, Fusion Eng. Des. **146**, 676 (2019).
[12] A. Zamengo and M. Agostini, "RF breakdowns in the SPIDER experiment during its first operational phase," paper presented at the MeVArc, 2019.
[13] B. Heinemann *et al.*, Fusion Eng. Des. **136**, 569 (2018).
[14] M. Siragusa *et al.*, "Numerical simulation of experimental tests performed on ZAO® non-evaporable-getter pump designed for NBI applications," paper presented at the ICIS, 2019 [Rev. Sci. Instrum. **91**, 023501 (2020)].
[15] E. Sartori *et al.*, Fusion Eng. Des. **151**, 111398 (2020).
[16] M. Pavei *et al.*, "SPIDER plasma grid masking for reducing gas conductance and pressure in the vacuum vessel," paper presented at the ISFNT, 2019 [Fusion Eng. Des. (submitted)].
[17] A. Maistrello *et al.*, "Voltage hold off test of the insulating supports for the plasma grid mask of SPIDER," paper presented at the ISFNT, 2019 [Fusion Eng. Des. (submitted)].
[18] R. Pasqualotto *et al.*, J. Instrum. **12**, C10009 (2017).
[19] R. Pasqualotto *et al.*, AIP Conf. Proc. **1869**, 030020 (2017).
[20] M. Brombin *et al.*, Rev. Sci. Instrum. **85**, 02A715 (2014).
[21] M. Barbisan *et al.*, Fusion Eng. Des. **146**, 2707 (2019).
[22] A. Luchetta *et al.*, Fusion Eng. Des. **146**, 500 (2019).
[23] R. Pasqualotto *et al.*, Fusion Eng. Des. **146**, 709 (2019).
[24] B. Zaniol *et al.*, Rev. Sci. Instrum. **91**, 013103 (2020).
[25] P. Franzen *et al.*, Plasma Phys. Controlled Fusion **56**, 025007 (2014).
[26] R. Pasqualotto *et al.*, Fusion Eng. Des. **88**, 1253 (2013).
[27] A. Pimazzoni *et al.*, "Assessment of the SPIDER beam features by diagnostic calorimetry and thermography," paper presented at the ICIS, 2019 [Rev. Sci. Instrum. (in press)].
[28] E. Sartori *et al.*, Plasma Fusion Res. **13**, 3405092 (2018).
[29] C. Poggi *et al.*, "Design and development of an Allison type emittance scanner for the SPIDER ion source," paper presented at the ICIS, 2019 [Rev. Sci. Instrum. **91**, 013328 (2020)].
[30] S. Cristofaro *et al.*, Rev. Sci. Instrum. **90**, 113504 (2019).
[31] M. Barbisan *et al.*, J. Instrum. **14**, C12011 (2019).
[32] E. Sartori, "Simulation-based quantification of alkali-metal evaporation rate and systematic errors from current-voltage characteristics of Langmuir-Taylor detectors," IEEE Trans. Instrum. Meas. (to be published).
[33] M. Fadone *et al.*, "Interpreting the dynamic equilibrium during evaporation in a Caesium environment," paper presented at the ICIS, 2019 [Rev. Sci. Instrum. **91**, 013332 (2020)].
[34] R. H. S. Hemsworth *et al.*, New J. Phys. **19**, 025005 (2017).
[35] P. Agostinetti *et al.*, Nucl. Fusion **56**, 016015 (2016).
[36] V. Toigo *et al.*, Nucl. Fusion **59**, 086058 (2019).
[37] H. Tobari *et al.*, "Completion of DC 1 MV power supply system for ITER neutral beam test facility," in Preprint: 2018 IAEA Fusion Energy Conference, Gandhinagar, India, 22–27 October 2018, FIP/1-10.
[38] L. Zanotto *et al.*, Fusion Eng. Des. **146**, 2238 (2019).
[39] A. Maistrello *et al.*, Fusion Eng. Des. **131**, 96 (2018).
[40] N. Pilan *et al.*, Fusion Eng. Des. **88**, 1038 (2013).
[41] M. Cavenago *et al.*, Rev. Sci. Instrum. **91**, 013316 (2020).